Universal enhancement of superconductivity in two dimensional semiconductors at low doping by electron-electron interaction.

Matteo Calandra,* Paolo Zoccante, and Francesco Mauri†
IMPMC, UMR CNRS 7590, Sorbonne Universités - UPMC Univ. Paris 06, MNHN, IRD, 4 Place Jussieu, F-75005 Paris, France

In 2-dimensional multivalley semiconductors, at low doping, even a moderate electron-electron interaction enhances the response to any perturbation inducing a valley polarization. If the valley polarization is due to the electron-phonon coupling, the electron-electron interaction results in an enhancement of the superconducting critical temperature. By performing first principles calculations beyond DFT, we prove that this effect accounts for the unconventional doping-dependence of the superconducting transition-temperature (T_c) and of the magnetic susceptibility measured in Li_xZrNCl. Finally we discuss what are the conditions for a maximal T_c enahnacement in weakly doped 2-dimensional semiconductors.

arXiv:1408.6502v2 [cond-mat.supr-con] 13 Jan 2015

The quest for high T_c superconductivity has mainly focused on strongly correlated materials in proximity of electronic instabilities like the Mott transition (cuprates [1]) or fragile magnetic states (iron pnictides [2, 3]). Heavily doped three dimensional (3D) covalently bonded semiconductors, like diamond [4], silicon [5] and SiC [6, 7] have been considered as an alternative, that, however, has lead, so far, to fairly low T_c (< 10 K). In 3D, the density of states at the Fermi level slowly grows with doping. As T_c increases with the density of states [8], a large number of carriers has to be introduced to achieve a large T_c. This demanding requirement could be released in 2 dimensional (2D) semiconductors, such as transition metal dichalcogenides [9–12], cloronitrides [13, 14] or other layered materials with massive Dirac fermions, where the doping can be controlled by intercalation [13, 14] or field-effect [11, 12, 15]. In 2D, the density of states is a constant function of the Fermi energy (ϵ_F) and, in principle, T_c is expected to be insensitive on doping. Surprisingly, measurements on Li_xZrNCl [13, 14, 16], a weakly-doped multivalley 2D semiconductor, revealed that T_c not only does not increase with doping but even decreases. Here we show that the e-e interaction is responsible for such a puzzling behavior. In particular, in a weakly-doped 2D multivalley semiconductor, e-e manybody effects enhance the response to any perturbation inducing a valley polarization. If the valley polarization is due to the electron-phonon coupling, the e-e interaction will lead to a large increase of T_c. We demonstrate that this effect explains the high T_c in Li_xZrNCl and its unconventional behavior [16] as a function of doping. Finally, by finding the conditions for a maximal Tc enhancement, we show how weakly-doped 2D semiconductors are an alternative route towards high Tc superconductivity.

The electronic structure of multivalley semiconductors has minima (maxima) in the conduction (valence) band that are named valleys. In the low doping limit, the equivalent g_v valleys are occupied by few electrons or holes and the electronic structure is described by the effective mass theory. The resulting model Hamiltonian is that of a multicomponent electron gas of mass m^* and density n where the valley index plays the role of a pseudospin. Since at low doping the Fermi momentum κ_F, as measured from the valley bottom, is much smaller than the valley separation, the intravalley e-e interaction dominates over the intervalley one, and (for an isotropic mass tensor) the manybody Hamiltonian has $SU(2g_v)$ symmetry in valley and spin indexes [5, 17, 19, 20]. In 2D the intravalley Coulomb interactions is $2\pi/(\epsilon_M q)$, where q is the exchanged momentum, and ϵ_M the environmental dielectric constant. The strength of e-e scatteringis measured by the parameter $r_s = 1/(a_B\sqrt{\pi n})$ where $a_B = \epsilon_M \hbar^2/(m^* e^2)$.

The magnetic properties of a doped semiconductor are described by the interacting spin susceptibility, χ_s:

$$\chi_s = \frac{\partial M}{\partial B_{\rm ext}} \tag{1}$$

where M and $B_{\rm ext}$ are the spin magnetization and the external magnetic field. The non-interacting spin susceptibility is doping independent, namely $\chi_{0s} = \mu_S^2 N(0)$, where μ_S is the electron-spin magnetic moment and $N(0) = g_v m^*/(\pi\hbar^2)$ the density of states at ϵ_F. Manybody e-e effects increase χ_s with respect to its non-interacting value χ_{0s} and can lead to a magnetic state. Indeed the e-e energy is lower in the spin-polarized state, since electrons with same spin and valley cannot occupy same spatial position because of the Pauli exclusion principle. The enhancement χ_s/χ_{0s} increases with increasing r_s (as the relative contribution of exchange to the total energy increases) and it is significant already at moderate correlations, $r_s \approx 1$ [4, 19, 20, 22, 23].

In a multivalley electron gas, an external perturbation can induce a valley polarization. The existence of such a valley polarization in 2D systems is at the heart of recent developments in the field of valleytronics [10], the valley analogue of spintronics. Any perturbation inducing an asymmetry in the population of the different valleys can then be seen as an external pseudo magnetic field. In analogy with the magnetic case, a valley susceptibility

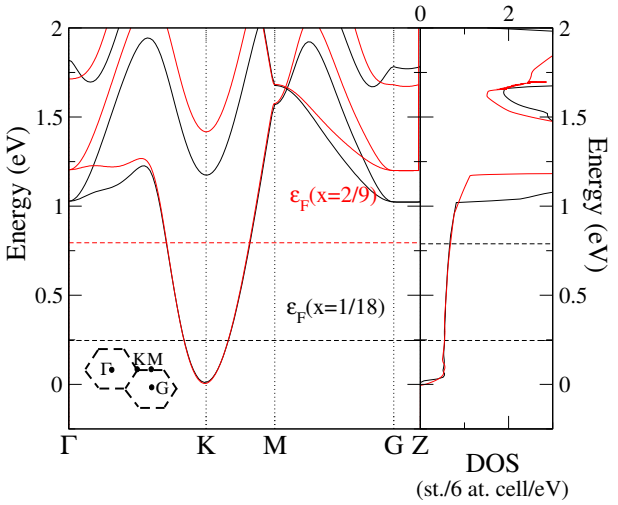

FIG. 1. Electronic structure and density of states of Li_xZrNCl for $x = 1/18$ (black) and $x = 2/9$, (red).

χ_v is defined as the first derivative of the valley magnetization (μ_s times the valley-population difference) with respect to the external pseudo magnetic field.

In the low doping limit, because of the SU($2g_v$) valley-spin symmetry of the model Hamiltonian [5, 19, 20], the valley susceptibility χ_v is equal to the spin susceptibility χ_s. This equality was experimentally verified in AlAs quantum wells [24] where the pseudo magnetic field was generated by a strain deformation. Similarly to the strain case in AlAs, an intervalley phonon can also act as a pseudo magnetic field by inducing a valley splitting and a valley polarization via the electron-phonon interaction. As a consequence, the manybody enhancement of the valley susceptibility can result in an augmentation of the superconducting critical temperature (T_c) at low doping, as we show it happens in Li_xZrNCl.

ZrNCl is a layered large gap semiconductor, with an extremely weak interlayer coupling ($t_\perp < 1.5$ meV) and 2 equivalent valleys with isotropic mass tensors in the conduction band (see Fig. 1 (a)) at the special points $\mathbf{K}$ and $\mathbf{K'} = 2\mathbf{K}$. The Li intercalation acts as a rigid filling of the conduction band with x electrons [25]. The bands are almost parabolic with $m^* = 0.57$ (in units of e mass) for doping $x \leq 2/9$ (see Fig. 1 (a)). Li_xZrNCl is thus a realisation of a 2D 2-valley electron-gas. The system remains insulating due to an Anderson localization for $x \leq 0.05$ and then becomes superconducting at larger doping [13]. The spin-susceptibility χ_s increases as doping is reduced, as shown in Fig. 2 (top-panel). As the non-interacting χ_{0s} is doping independent in 2D, this increase can only be due to exchange-correlation effects. The superconducting T_c behaves similarly to χ_s as it *increases* from 11.5 K to 15 K for x *decreasing* from 0.3 to 0.05 (see Fig. 2 bottom panel and Ref. [16]), suggesting that the two effects are related.

In order to evaluate the interacting χ_s, we consider a 2D 2 valley electron-gas with a finite thickness equal to that of the ZrN layer and environmental dielectric constant $\epsilon_M = 5.59$, as calculated density functional theory (DFT) for the insulating compound ZrNCl [26]. We obtain the χ_s/χ_{0s} enhancement in the random-phase approximation (RPA) [17]. The RPA closely reproduces the quantum Monte-Carlo results [4, 19, 22], for r_s values relevant for Li_xZrNCl ($r_s < 1.5$). As shown in Fig. 2 central panel, the enhancement is already large at these intermediate values of r_s. To compare with measurements, we add to our χ_s a constant C that takes into account the doping-independent Landau diamagnetic terms (see Eq. 4 in [17]) present in the experimental data. Our χ_s closely reproduces the dependence on doping measured in experiments [1, 17].

In a Fermi liquid approach, the electron-phonon coupling parameter of a mode ν at a phonon-momentum $\mathbf{q}$ is given by:

$$\widetilde{\lambda}_{\mathbf{q}\nu} = \frac{2}{\omega^2_{\mathbf{q}\nu} N(0) N_k} \sum_{\mathbf{k}} |\widetilde{d}^{\nu}_{\mathbf{k},\mathbf{k}+\mathbf{q}}|^2 \delta(\epsilon_{\mathbf{k}}) \delta(\epsilon_{\mathbf{k}+\mathbf{q}}) \quad (2)$$

where the tilde indicates that the quantities are fully screened by all kind of exchange-correlation interaction (charge, spin and valley). The quasiparticle energies are $\epsilon_{\mathbf{k}}$ and $\widetilde{d}^{\nu}_{\mathbf{k},\mathbf{k}+\mathbf{q}} = \langle \mathbf{k}|\delta\widetilde{V}/\delta u_{\mathbf{q}\nu}|\mathbf{k}+\mathbf{q}\rangle$, with $\widetilde{V}$ being the screened [7] single-particle potential that includes, at the mean-field level, the e-e interaction [29]. Moreover $u_{\mathbf{q}\nu}$ and $\omega_{\mathbf{q}\nu}$ are the phonon displacement and frequency. In GGA or LDA functionals the exchange-correlation energy depends explicitly on charge densities and spin polarization, but not on valley polarizations. As a consequence the SU(4) spin and valley symmetry of the manybody Hamiltonian is broken. Thus the matrix elements in Eq. 2 do not include any enhancement due to intervalley exchange-correlation [17]. They are then undressed (bare) with respect to intervalley exchange-correlation interaction. We label them as $d^{\nu}_{\mathbf{k},\mathbf{k}+\mathbf{q}}$ and $\lambda_{\mathbf{q}\nu}$, without the tilde. In the Hartree-Fock (HF) approximation, the matrix elements include an intervalley exchange-correlation enhancement, that is, however, severely overestimated with respect to Quantum Monte Carlo or RPA results [19]. For this reason, hybrid functional calculations [30] lead to matrix elements $\widetilde{d}^{\nu}_{\mathbf{k},\mathbf{k}+\mathbf{q}}$ that crucially depends on the amount of HF exchange included.

To evaluate the bare quanty $\lambda_{\mathbf{q}\nu}$ as a function of doping, we use DFT [32] and Wannier interpolation [7] (see [17] for other doping). We find a marked softening of an intervalley phonon having ≈ 59 meV phonon-energy at $x = 1/18$ in a region of radius $2\kappa_F$ around $\mathbf{K}$ (Fig. 3). As the softening $\Delta\omega_{\mathbf{q}\nu}$ is essentially constant in this region, we conclude that $|d^{\nu}_{\mathbf{k},\mathbf{k}+\mathbf{K}}| \approx |d^{\nu}_{\mathbf{K},2\mathbf{K}}|$. Indeed, under this assumption the phonon softening at $\mathbf{q}$ close to $\mathbf{K}$ is $\Delta\omega_{\mathbf{q}\nu} \approx -\chi_0(\mathbf{q})|d^{\nu}_{\mathbf{K},2\mathbf{K}}|^2/(2\omega_{\mathbf{q}\nu})$ [17]. Here $\chi_0(\mathbf{q})$ is the bare finite-momentum response-function,

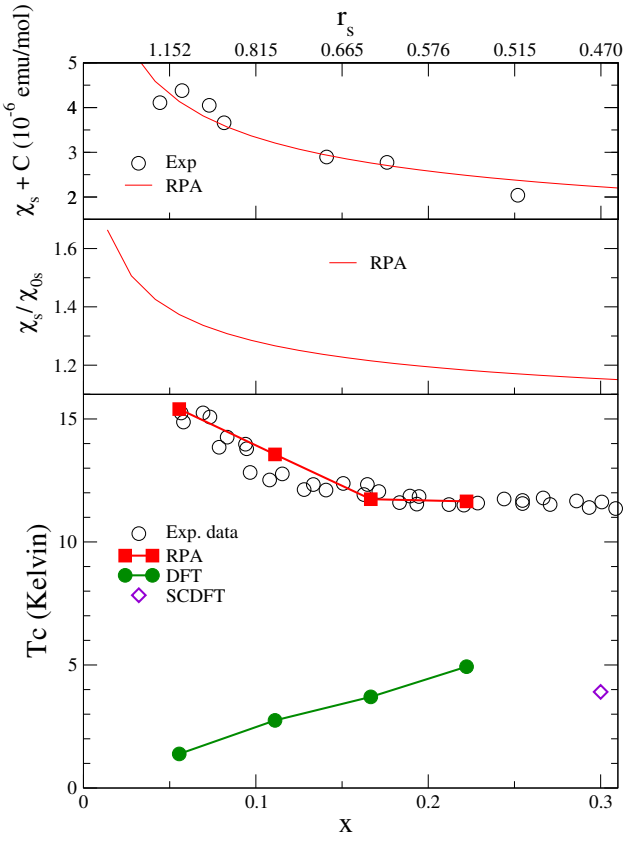

FIG. 2. Top: Spin susceptibility (χ_s) calculated in the random phase approximation (RPA) and experimental susceptibility. The experimental data from Ref. [1] have been corrected for an erroneous estimate of the Landau diamagnetic susceptibility, χ_L, (see sec. A in [17] and supplementary materials in Ref. [1]). Center: RPA enhancement factor (χ_s/χ_{0s}). Bottom: Experimental [1] and calculated T_c using different approximations. The Superconducting Density Functional Theory calculation is from Ref. [31]

which is constant and doping independent in 2D for $|\mathbf{q}-\mathbf{K}| < 2\kappa_F$ [17, 33].

The average electron-phonon coupling λ as a function of doping is shown in Tab. I. We further decompose λ in inter- and intra-valley contributions finding that at low doping (i) the intravalley contribution is suppressed for x going to zero and (ii) the intervalley contribution is almost doping independent and dominant, as shown in Fig. 3 and in [17]. In the Eliashberg function at $x = 1/18$ most of the coupling arises from intervalley phonons at ≈ 59 and 24.5 meV, (Fig. 3). These phonons have large phonon linewidths $\gamma_{\mathbf{q}\nu} = \pi N(0)\omega^2_{\mathbf{q}\nu}\lambda_{\mathbf{q}\nu}$, as shown by the red bars in Fig. 3. Finally, both the average electron-phonon coupling and the logarithmic average of the phonon frequencies are roughly constant (see Tab. I), so that T_c as obtained from McMillan equation [34] slightly increases with doping, in agreement with previous calculations at higher doping [25, 31], but in qualitative disagreement with experimental data (see Fig. 2 bottom panel).

Assuming a constant intravalley electron-phonon matrix element ($|d^\nu_{\mathbf{k},\mathbf{k}+\mathbf{K}}| \approx |d^\nu_{\mathbf{K},\mathbf{2K}}|$), we can derive an effective Hamiltonian where the presence of a small phonon displacement $u_{\mathbf{K}\nu}$ is described as an external pseudo magnetic field $B^\nu_{\rm ext} = |d^\nu_{\mathbf{K},\mathbf{2K}}|u_{\mathbf{K}\nu}/\mu_S$. Indeed, if we define a 2-component spinor using as basis the states $|\mathbf{K}+\boldsymbol{\kappa}\rangle$ and $|2\mathbf{K}+\boldsymbol{\kappa}\rangle$, where $\boldsymbol{\kappa} = \mathbf{k}-\mathbf{K}$, we obtain the following form of the one-body part of the Hamiltonian:

$$H^\nu_{\boldsymbol{\kappa}} = \frac{\hbar^2\kappa^2}{2m^*}\hat{I} + B^\nu_{\rm ext}\,\mu_S\hat{\sigma_x}, \tag{3}$$

where $\hat{I}$ and $\hat{\sigma_x}$ are the 2×2 identity and the Pauli matrix along the x-direction, respectively. Here, without loss of generality, B^ν_{ext} has be chosen to be real by fixing appropriately the relative phase between the $|\mathbf{K}+\boldsymbol{\kappa}\rangle$ and $|\mathbf{2K}+\boldsymbol{\kappa}\rangle$ states (see sec. G in [17]).

We explicitly verify the accuracy of such Hamiltonian by performing a DFT electronic structure calculations on a $\sqrt{3}\times\sqrt{3}$ supercell with AA stacking. In this supercell, the 2 valleys at $\mathbf{K}$ and $2\mathbf{K}$ in the unit cell, are folded at the zone center. As shown in Fig. 4, by displacing the atoms from the equilibrium, the intervalley phonon splits the 2 valleys by a constant amount equal to $2B^\nu_{\rm ext}\mu_S$, as predicted by the model Hamiltonian. The intervalley phonons induce a valley polarization and act as a pseudo magnetic field. As it happens in the magnetic case, the response to the pseudo magnetic field is enhanced by the intervalley exchange-correlation (which is however absent in our DFT calculation, as shown in [17]). As the total magnetization due to the pseudo magnetic field $B^\nu_{\rm ext}$ is written either as $M = \chi_s B^\nu_{\rm ext}$ or as $M = \chi_{0s}\widetilde{B}^\nu$, where now $\widetilde{B}^\nu$ is the total magnetic field, sum of the external plus the exchange-correlation field, we have [17],

$$\frac{\widetilde{B}^\nu}{B^\nu_{\rm ext}} = \frac{|\widetilde{d}^\nu_{\mathbf{K},\mathbf{2K}}|}{|d^\nu_{\mathbf{K},\mathbf{2K}}|} = \frac{\chi_s}{\chi_{0s}} \tag{4}$$

namely the electron-phonon coupling at $\mathbf{q}=\mathbf{K}$ is renormalized by intervalley correlation effects exactly in the same way as the spin susceptibility with an enhancement that is independent from the phonon index ν. Assuming again a constant intervalley matrix element we have that:

$$\tilde{\lambda}^{\rm inter} = \left(\frac{\chi_s}{\chi_{0s}}\right)^2 \lambda^{\rm inter} \tag{5}$$

so that $\tilde{\lambda} = \lambda^{\rm intra} + \tilde{\lambda}^{\rm inter}$. We use the χ_s/χ_{0s} of Fig. 2 (central panel) to evaluate $\tilde{\lambda}$, the renormalized Eliashberg function and T_c using McMillan equation [34]. The results are shown in Fig. 2 (bottom panel). We now find that the doping dependence of T_c is in excellent agreement with experimental data. In addition, by using a reasonable value of μ we also obtain T_c in agreement with experiments. Intervalley exchange-correlation is the mechanism responsible for the enhancement of T_c at low doping in Li_xZrNCl.

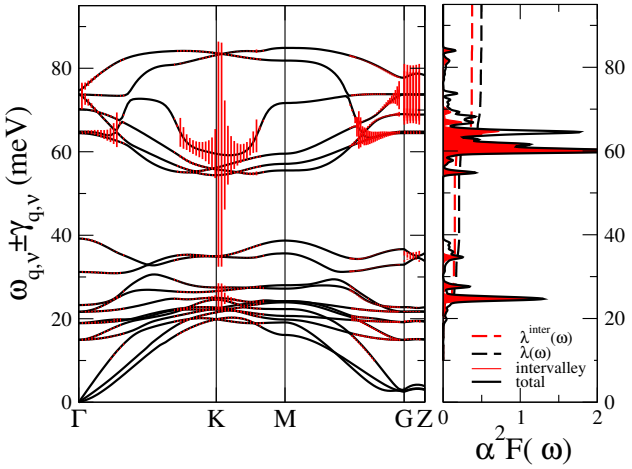

FIG. 3. Phonon dispersion, phonon linewidth (red bars) and Eliashberg function of $Li_{1/18}ZrNCl$. The Eliashberg function due to intervalley coupling only is shown as the filled region in the right panel (see [17] for other doping).

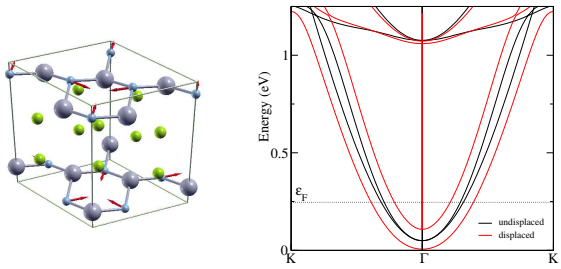

FIG. 4. (a) Phonon displacements of the 59 meV modes at **K** in a $\sqrt{3} \times \sqrt{3}$ supercell with AA stacking. (b) Effect of the phonon displacements in (a) on the electronic structure of the $\sqrt{3} \times \sqrt{3}$ supercell with AA stacking. The dotted line labels ϵ_F. The point **K** is folded at **Γ** in the supercell. The displacements of the Zr and N atoms are 4×10^{-3}Å and 59×10^{-3}Å.

Here we have shown that the e-e interaction enhances T_c at low doping in Li_xZrNCl. Such finding is universal and provides a general guideline to realize a superconducting state in a doped semiconductor. First of all the system should be strongly 2D . In this case the density of states is doping independent and constant down to very low doping, where Anderson localization occurs. In three dimensional multivalley doped semiconductors, the enhancement of the valley susceptibility due to many-body effects still occurs, but the density of states tends to zero at low doping and T_c is suppressed [4–7]. Furthermore, in order for the enhancement to occur, a multivalley electronic structure is needed but 2 is the optimal number of valleys. Indeed, the enhancement is smaller as the number of valleys increases and ultimately tends to one in the limit of infinite number of valleys. Finally, the T_c enhancement is larger, the larger the r_s parameter. A larger r_s parameter can be obtained reducing the doping, reducing the dielectric constant of the spacers (ϵ_M) or increasing m^*. At fixed ϵ_M and m^*, the largest enhancement should be found in the proximity of the band insulating or semiconducting state. In the very low doping limit, in the absence of disorder, the enhancement of T_c can be so large to induce high T_c superconductivity. However, in this limit, disorder and the resulting Anderson localization tend to suppress superconductivity. Thus, high T_c superconductivity will only be seen in very clean samples. Finally, it is worth to recall than the pairing mechanism does not need to be necessary the electron-phonon interaction. Indeed, any mechanism (e.g. spin-fluctuations) inducing a valley polarization will experience an enhancement of T_c due to intervalley exchange-correlation.

TABLE I. ϵ_F, $\omega_{\log}$, λ, $\omega_{\log}^{\rm intra}$, $\lambda^{\rm intra}$, $\omega_{\log}^{\rm inter}$,$\lambda^{\rm inter}$ from DFT. Energies in meV. The enhancement χ_v/χ_{0v} is calculated in the RPA approximation. The couplings $\widetilde{\lambda}^{\rm inter}$ and $\widetilde{\lambda}$ are obtained via Eq. 5.

x	ϵ_F	$\omega_{\log}$	λ	$\omega_{\log}^{\rm intra}$	$\lambda^{\rm intra}$	$\omega_{\log}^{\rm inter}$	$\lambda^{\rm inter}$	$\frac{\chi_v}{\chi_{0v}}$	μ^*	$\widetilde{\lambda}$
1/18	246	43.9	0.48	48.0	0.10	42.8	0.38	1.37	0.165	0.82
1/9	448	44.8	0.51	47.6	0.11	43.9	0.39	1.27	0.150	0.74
1/6	622	44.6	0.52	45.5	0.16	44.3	0.36	1.21	0.143	0.69
2/9	790	43.3	0.55	42.9	0.20	43.4	0.35	1.18	0.138	0.69

We acknowledge discussions with M. L. Cohen ,S. de Palo, R.Heid, M. Johannes, I. I. Mazin and S. Moroni, and support from the Graphene Flagship and by ANR-11-BS04-0019 and ANR-13-IS10-0003-01. Computer facilities were provided by CINES, CCRT and IDRIS.

* matteo.calandra@upmc.fr
† francesco.mauri@upmc.fr

[1] J. G. Bednorz, K. A. Mueller Zeitschrift für Physik B , **64** 189, (1986)
[2] Kamihara Y., *et al.* , J. Am. Chem. Soc. **128** 10012 (2006)
[3] R. S. Dhaka *et al.*, Phys. Rev. B **89**, 020511(R) (2014)
[4] Ekimov, E. A. et al., Nature **428**, 542 (2004)
[5] Bustarret, E. et al., Nature **444**, 465 (2006).
[6] Ren, Z.-A. et al., J. Phys. Soc. Jap. **76**, 103710 (2007)
[7] Kriener,M., Maeno,Y., Oguchi,T., Ren,Z.A., Kato,J., Muranaka,T., Akimitsu,J. Phys. Rev. B **78**, 024517 (2008).
[8] E. Bustarret et al., Phys. Rev. Lett. 93, 237005 (2004).
[9] Novoselov K. S., Jiang D., Schedin F., Booth T. J., Khotkevich V. V., Morozov S. V. and A. K. Geim, PNAS **102**, 10451 (2005)
[10] Xiaodong Xu, Wang Yao, Di Xiao, Tony F. Heinz, Nature Physics **10**, 343–350 (2014).
[11] Zhang Y. J., Oka T., Suzuki R., Ye, J.T. and Iwasa, Science **344**, 725 (2014)
[12] Ye J. T., Zhang, Y. J., Akashi R., Bahramy, M. S., Arita R, and Iwasa Y, Science **338**, 1193 (2012)

[13] S. Yamanaka, H. Kawaji, K. Hotehama, and M. Ohashi, Advanced Materials **8**, 771 (1996).

[14] Yamanaka S., Hotehama K. and Kawaji H., Nature **392**, 580 (1998)

[15] J. T. Ye, S. Inoue, K. Kobayashi, Y. Kasahara, H. T. Yuan, H. Shimotani, and Y. Iwasa, Nature Materials **9**, 125 (2010)

[16] Y. Taguchi, A. Kitora, and Y. Iwasa, Phys. Rev. Lett. **97**, 107001 (2006)

[17] See supplementary materials joined in the submission which includes references [1–6].

[18] Ando T., Fowler A. B., and Stern F., Rev. Mod. Phys. **54**, 437 (1982)

[19] M. Marchi, S. De Palo, S. Moroni, and G. Senatore, Physical Review B, **80**, 035103 (2009)

[20] S. Das Sarma, E. H. Hwang, and Qi Li, Phys. Rev. B **80**, 121303(R) (2009)

[21] Y. Zhang and S. Das Sarma, Physical Review B, **72** , 075308 (2005)

[22] Y. Zhang and S. Das Sarma, Physical Review B, **72** 115317 (2005).

[23] C. Attaccalite, S. Moroni, P. Gori-Giorgi, and G. B. Bachelet, Physical Review Letters, **88** , 256601 (2002)

[24] O. Gunawan, Y. P. Shkolnikov, K. Vakili, T. Gokmen, E. P. De Poortere, and M. Shayegan, Physical Review Letters, **97** 186404 (2006)

[25] R. Heid and K. P. Bohnen, Phys. Rev. B **72**, 134527 (2005)

[26] A. Kaur, E. R. Ylvisaker, Y. Li, G. Galli, and W. E. Pickett, Phys. Rev. B 82, 155125 (2010)

[27] Y. Kasahara, T. Kishiume, T. Takano, K. Kobayashi, E. Matsuoka, H. Onodera, K. Kuroki, Y. Taguchi, and Y. Iwasa, Phis. Rev. Lett. **103**, 077004 (2009)

[28] M. Calandra, G. Profeta, and F. Mauri, Phys. Rev. B **82**, 165111 (2010)

[29] The matrix element $d_{\mathbf{k},\mathbf{k+q}}$ is related to the conventional electron-phonon matrix element $g_{\mathbf{k},\mathbf{k+q}}$ by the relation, $d_{\mathbf{k},\mathbf{k+q}} = g_{\mathbf{k},\mathbf{k+q}}\sqrt{2\omega_{\mathbf{q}\nu}}$.

[30] Z. P. Yin, A. Kutepov and G. Kotliar, Phys. Rev. X **3**, 021011 (2013)

[31] R. Akashi, K. Nakamura, R. Arita, and M. Imada Phys. Rev. B **86**, 054513 (2012)

[32] The results reported in the present paper were obtained from first-principles DFT in the linear response as implemented in the QUANTUM-ESPRESSO [37] package. Converged phonon dispersion and electron-phonon interaction were obtained by using Wannier interpolation [7]. Li intercalation was simulated by changing the number of electrons and adding a jellium compensating background [25]. All the structures considered were obtained by using the experimental lattice parameters and performing optimization of internal coordinates. More details in [17].

[33] Giuliani G. F. and Vignale G., Cambridge (2005)

[34] The superconducting critical temperature was estimated using the Allen-Dynes formula[38]. We choose the value of the unscreened Coulomb pseudopotential[35, 36] ($\mu = 0.198$) that leads to the correct estimate of T_c at the highest doping $x = 2/9$ by using the RPA renormalized electron-phonon coupling $\tilde{\lambda}$. This value is also close to the GW estimate of 0.203 computed at x=0.1 in Ref. [31] (page 13, middle second column). We then obtain μ^* at any doping from $\mu^* = \mu/(1+\mu\log(\epsilon_f/\omega_D))$, where ϵ_f and $\omega_D = 90$ meV are the Fermi level and the Debye energy respectively.

[35] P. Morel and P. W. Anderson, Phys. Rev. **125**, 1263 (1962)

[36] N. N. Bogoliubov, V. V. Tolmachev, and D. V. Shirkov, *A New Method in the Theory of Superconductivity* (1958) (translation: Consultants Bureau, Inc. , New York, 1959)

[37] P. Giannozzi *et al.*, J. Phys. Condens. Matter **21**, 395502 (2009).

[38] P. B. Allen and R. C. Dynes, Phys. Rev. B **12**, 905 (1975)

[39] G. Vignale, M. Rasolt and D. J. W. Geldart, Phys. Rev. B **37**, 2502 (1988)

[40] G. Vignale, M. Rasolt, Phys. Rev. Lett. **59**, 2360 (1987).

[41] Ando T., Fowler A. B., and Stern F., Rev. Mod. Phys. **54**, 437 (1982)

[42] O. Gunnarsson and B. I. Lundqvist, Phys. Rev. B **13**, 4274 (1976)

Supplementary Materials of

Weakly-doped two-dimensional semiconductors: a new route towards high T_c superconductivity.

Spin susceptibility from experiments

Experiments do not measure directly the spin-susceptibility of conduction electrons, but the sum of orbital and spin contributions of *all* the electrons present in the system. The contributions of non-conducting electrons and the orbital contribution of conducting electrons (Landau susceptibility, see discussion below) are doping independent. Thus, the raw experimental susceptibility data cannot be compared directly with the spin susceptibility of conduction electrons.

For this reason in Ref. [1] (see, in particular, the discussion in the supplementary information of Ref. [1]) all possible diamagnetic contributions where subtracted from the measured susceptibility χ, namely:

$$\chi_s = \chi - \chi_{\rm core}^{\rm Li^+} - \chi_{\rm core}^{\rm ZrNCl} - \chi_L - \chi_{orb} \tag{6}$$

where $\chi_{\rm core}^{\rm Li^+}$ and $\chi_{\rm core}^{\rm ZrNCl}$ are the core diamagnetic susceptibility from Li ion and pristine $\beta-$ZrNCl, respectively. The quantities χ_L and $\chi_{\rm orb}$ are the Landau diamagnetic and orbital susceptibilities, respectively. The $\chi_{\rm core}^{\rm Li^+}$ and $\chi_{\rm core}^{\rm ZrNCl}$ susceptibilities are doping independent. The orbital susceptibility $\chi_{\rm orb}$ was considered zero for a magnetic field applied along the c direction. Finally, in Ref. [1] the Landau susceptibility χ_L was assumed to be

$$\chi_L = -\frac{1}{3m^*}\chi_s \tag{7}$$

where m^* is the band effective mass in units of the electron mass ($m^* = 0.66$ in [1]). This last assumption is not correct. Indeed, in a 2D electron gas with parabolic bands:

$$\chi_{0L} = -\frac{1}{3(m^*)^2}\chi_{0s} \tag{8}$$

where χ_{0L} is the non interacting Landau susceptibility. Moreover, it has been shown that many-body effects strongly renormalize the spin susceptibility, while the Landau susceptibility is only weakly renormalized [2, 3]. For the doping regime considered here we can assume that $\chi_{0L} = \chi_L$. Thus Eq. 7 should be replaced by:

$$\chi_L = -\frac{1}{3(m^*)^2}\chi_{0s} = -\frac{\mu_S^2}{3(m^*)^2}N(0). \tag{9}$$

Since we are only interested in the variation of the susceptibility with doping, and χ_{0s} is doping independent, we add back to the experimental data the negative quantity, erroneously removed with Eq. 7. This is done by multiplying the susceptibilities presented in Fig. 4 of Ref. [1] by a $[1-1/(3m^*)] = 0.495$ factor. The results are reported in Fig. 2 in our main paper as measured data.

Model Hamiltonian and SU($2g_v$) spin-valley symmetry in the low density limit

We consider an isolated band partially filled with electrons. Within this band, the electrons experience a Coulomb repulsion

$$v(q) = \frac{2\pi e^2}{\epsilon_M q} \tag{10}$$

where $\mathbf{q}$ is the exchanged momentum between the two interacting electrons. The effect of the screening of other (empty) conduction and (filled) valence bands is included via the environmental dielectric constant ϵ_M. We can define two types of electron-electron scattering: i) the intravalley scattering with $q \sim \kappa_F$ (κ_F being the Fermi momentum measured from the valley bottom), that does

not change the valley index of the electrons, ii) the intervalley scattering with $q \sim |\mathbf{K} - \mathbf{K}'| = |\mathbf{K}|$ ($\mathbf{K}$ and $\mathbf{K}' = 2\mathbf{K}$ being the positions of the valley bottoms in the Brillouin zone), that changes the valley index of the electrons.

In the low doping limit, namely for $\kappa_F \ll |\mathbf{K} - \mathbf{K}'|$, because of the divergence of the Coulomb repulsion for $q \to 0$, the intravalley scattering is dominant and the intervalley scattering can be neglected. Under this hypothesis, the valley index (as the spin index) is conserved by the Coulomb interaction, it can be treated as a pseudospin and the manybody Hamiltonian has exact SU($2g_v$) spin and valley symmetry, namely

$$H = \sum_{\boldsymbol{\kappa} v\sigma} \frac{\hbar^2\kappa^2}{2m^*} c^\dagger_{\boldsymbol{\kappa} v\sigma} c_{\boldsymbol{\kappa} v\sigma} + \sum_{\boldsymbol{\kappa} v\sigma} \sum_{\boldsymbol{\kappa}' v'\sigma'} \sum_{\boldsymbol{q}} v(q) c^\dagger_{\boldsymbol{\kappa} v\sigma} c^\dagger_{\boldsymbol{\kappa}' v'\sigma'} c_{\boldsymbol{\kappa}'-\boldsymbol{q} v'\sigma'} c_{\boldsymbol{\kappa}+\boldsymbol{q} v\sigma} \tag{11}$$

where $v, v' = 1, ..., g_v$ are valley indexes and $\sigma, \sigma' = \pm$ are spin indexes and c,$c^\dagger$ are creation and destruction operator (see e. g. Eq. 3.35 of Ref. [5]). The Hamiltonian in Eq. 11 holds as long as (i) the screening of the other bands can be included in the environmental dielectric constant, (ii) intervalley scattering can be neglected. If these two conditions are satisfied, then it holds regardless of the number of valleys and of their position in the Brillouin zone.

As the Hamiltonian in Eq. 11 has exact SU($2g_v$) spin and valley symmetry, it follows that:

$$\chi_v = \chi_s \tag{12}$$

Spin susceptibility in the random phase approximation

We compute the interacting spin susceptibility of a multivalley 2D electron gas in the random phase approximation. We integrate numerically the expression given by [4], which (after correcting few typos, namely, in [4], the 1 present on the r.h.s. of our equation below is missing and both the definitions of A and B are incorrect), reads:

$$\begin{aligned}\frac{\chi_{0s}}{\chi_s} = 1 - \frac{2\alpha r_s}{\pi}\int_0^1 dx \frac{xF(x)}{\sqrt{1-x^2}} + \frac{\sqrt{2}\alpha r_s}{\pi}\int_0^\infty x^2 F(x)dx \int_0^\infty du \left[\frac{1}{\epsilon(x,iu)} - 1\right] \\ \times \left(A\sqrt{1+A/R} - B\sqrt{1-A/R}\right) R^{-5/2}\end{aligned} \tag{13}$$

where $\alpha = \sqrt{g_v g_s/4}$ with g_v (g_s) being the valley (spin) degeneracy, $x = q/2k_F$, $A = x^4 - x^2 - u^2$, $B = 2x^2u$, $R = \sqrt{A^2 + B^2}$ and $u = \omega/(4\epsilon_F)$. The imaginary frequency dielectric function $\epsilon(x, iu)$ is defined as:

$$\epsilon(x, iu) = 1 + \alpha r_s g_v g_s F(x) \left[\frac{1}{2x} - \sqrt{A + R/(2^{3/2}x^3)}\right] \tag{14}$$

The wavefunctions of conduction bands are localized on ZrN bilayers. The thickness of each bilayer (distance between Zr and N along the z-axis) is $\approx 2.15\mathring{A}$. Considering the extension of the DFT charge density we set $a = 2.5$ Å.

In addition we also consider the perfect (long-range) metallic screening of the adjacent ZrN bilayers, located at a distance $d = 9.306$ Å. We encode this information in the form factor:

$$F(x) = \frac{2}{qa^*}(1 + \frac{e^{-qa^*} - 1}{qa^*}) + \frac{1 - e^{-4qd^*}}{1 + e^{-4qd^*} + 2e^{-2qd^*}} - 1 \tag{15}$$

where $q = 2xk_F$, $k_F = 1/(r_s\alpha)$, $a^* = a/a_B$, $d^* = d/a_B$, $a_B = (\epsilon_M/m^*)0.529177$ Å, and we suppose that $d \gg a$.

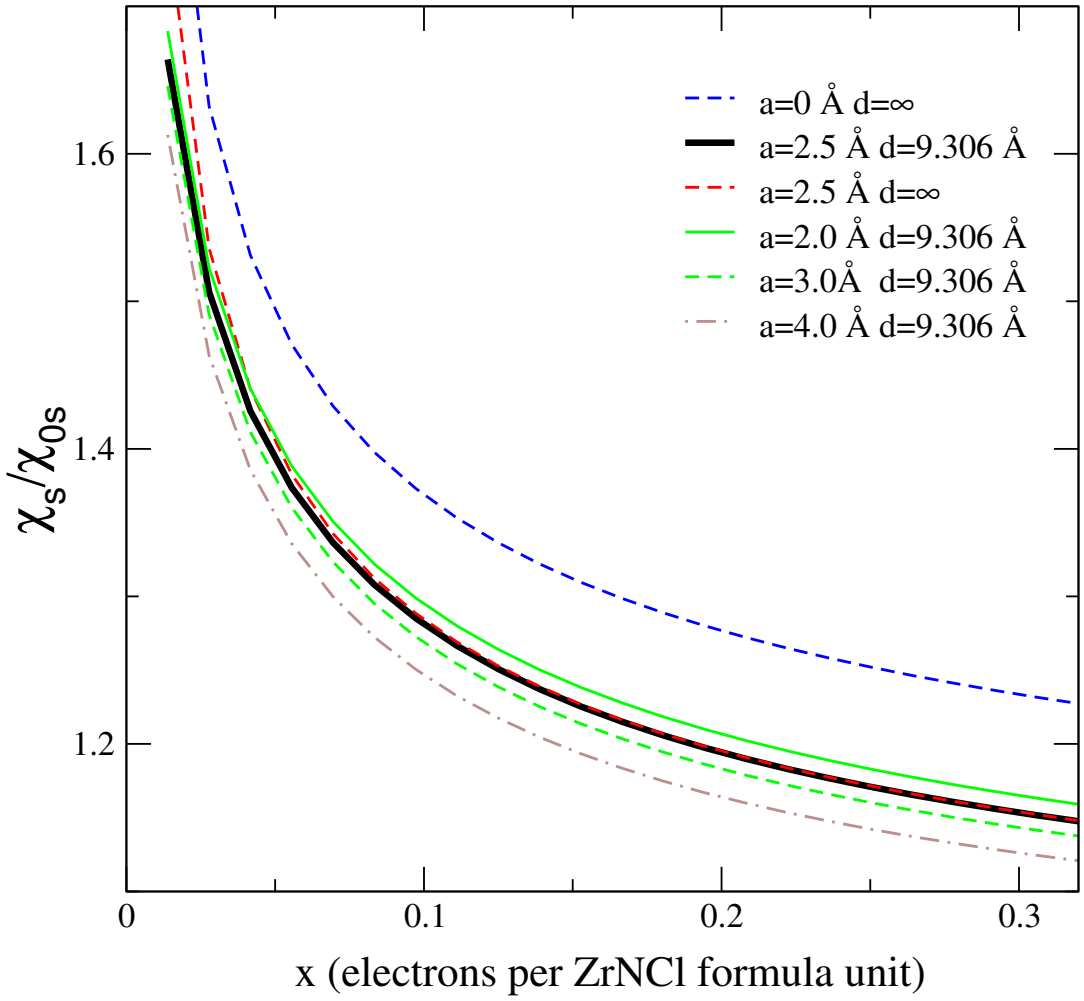

FIG. 5. Susceptibility enhancement as a function finite thickness a of the 2D electron-gas and of the interlayer distance d. In the main paper we report the results obtained with a=2.5 Å and d=9.306 Å.

The result of Eq. 13 are shown in Fig. 5. In the same picture we also compare the effect of the parameter a and of the metallic screening of the adjacent ZrN bilayers. The presence ($d = 9.306\AA$) or absence ($d = \infty$) of metallic screening has no influence on the ratio χ_s/χ_{0s}. Furthermore, the dependence on thickness is extremely weak for realistic values of a, namely $2 < a < 3$. The choice of this parameter is thus not critical.

In the top panel of Fig. 2 of our main paper, we add a doping independent constant C to the RPA result for χ_s to account for the Landau diamagnetic term, Eq. 9, and for the uncertainties on the estimations of the others diamagnetic (doping independent) terms of the left hand side of Eq 6. The best agreement with experiment is obtained for C$= -7.77 \times 10^{-6}$ emu/mol. Note that, using a value of $m^* = 0.57$ as in the rest of the paper, Eq. 9 gives $\chi_L = -8.89 \times 10^{-6}$ emu/mol, in close agreement with the value obtained for the constant C.

Spin susceptibility in local spin density functional theory

The total energy in local spin density functional theory in the presence of an external (bare) magnetic field $B_{\rm ext}$ is written as:

$$E_{LSD} = T + \int d\mathbf{r}\, \epsilon_{h,xc}(n,m) - \mu_s \int d\mathbf{r}\, m(\mathbf{r}) B_{\rm ext} \tag{16}$$

where T is the kinetic energy functional, $\epsilon_{h,xc}(n,m) = \epsilon_h(n) + \epsilon_{xc}(n,m)$ is the Hartree and exchange and correlation energy per particle, $n(\mathbf{r})$ is the electron density and $m(\mathbf{r}) = n_+(\mathbf{r}) - n_-(\mathbf{r})$. The Kohn-Sham potential for each spin channel ($\pm$) is written as

$$V_{KS}^{\pm} = \frac{\delta \epsilon_{h,xc}}{\delta n(\mathbf{r})} \pm \frac{\delta \epsilon_{h,xc}}{\delta m(\mathbf{r})} \mp \mu_s B_{\rm ext} \tag{17}$$

In a paramagnetic system[6], we have that

$$\left. \frac{\delta \epsilon_{xc}(n,m)}{\delta m} \right|_{m=0} = 0 \tag{18}$$

We can then expand at second order $\epsilon_{xc}(n,m)$ in m and obtain

$$V_{KS}^{\pm} = \frac{\delta \epsilon_{h,xc}}{\delta n(\mathbf{r})} \pm \frac{\delta^2 \epsilon_{xc}}{\delta m(\mathbf{r})^2}\, m \mp \mu_s B_{\rm ext}. \tag{19}$$

We call

$$\widetilde{B} = B_{\rm ext} + B_{xc} \tag{20}$$

the total (screened by the exchange-correlation) field, where

$$\mu_s B_{xc} = -\frac{\delta^2 \epsilon_{xc}}{\delta m(\mathbf{r})^2}\, m. \tag{21}$$

The fields are related to the magnetization by the following two relations:

$$\mu_s m = \chi_{0s} \widetilde{B}, \tag{22}$$

$$\mu_s m = \chi_s B_{\rm ext}. \tag{23}$$

where χ_{0s} and χ_s are the bare and interacting susceptibilities, respectively. Combining Eq.s 20, 21, and 23, we obtain:

$$\widetilde{B} = (1 - f\chi_s) B_{\rm ext} \tag{24}$$

where $f = \frac{\delta^2 \epsilon_{xc}}{\delta m(\mathbf{r})^2} \frac{1}{\mu_s^2} < 0$. From Eqs. 22 and 23 we have

$$\frac{\widetilde{B}}{B_{\rm ext}} = \frac{\chi_s}{\chi_{0s}} \tag{25}$$

meaning that the total magnetic field in the sample is renormalized by exchange-correlation effects exactly as the manybody enhancement of the spin susceptibility.

Replacing Eq. 25 in Eq. 24, we obtain:

$$\frac{\chi_s}{\chi_{0s}} = \frac{1}{1 + f\chi_{0s}} \tag{26}$$

The relation between the total (screened) magnetic field and the external (bare) one is determined by the function f that is related to the second derivative of the exchange correlation potential with respect to the spin magnetization. If the exchange correlation functional has no dependence on m, then $f = 0$ and there is no susceptibility enhancement.

Absence of valley susceptibility enhancement in local spin density

In Li_xZrNCl a valley polarization can be induced by the atomic displacements of an intervalley phonon, as shown in Fig. 4 in the main paper. In this case the deformation potential acts as an external (bare) $B^{\nu}_{\rm ext} = |d^{\nu}_{\mathbf{K},\mathbf{2K}}| u_{\mathbf{K}\nu}/\mu_S$ pseudo magnetic field.

In an exact many-body treatment, in the low doping limit, the $SU(4)$ spin and valley symmetry is preserved. This is not necessary the case if approximated local exchange and correlation functionals are used. If a 4-component local exchange correlation kernel is adopted in the calculation, namely

$$\epsilon_{xc} = \epsilon_{xc}(n, m, m_v) \tag{27}$$

where $m_v(\mathbf{r}) = n_{v=1}(\mathbf{r}) - n_{v=2}(\mathbf{r})$ is the valley magnetization and $\epsilon_{xc}(n, m, m_v) = \epsilon_{xc}(n, m_v, m)$, then the $SU(4)$ symmetry can be preserved. The valley exchange-correlation enhancement is written as

$$\frac{\chi_s}{\chi_{0s}} = \frac{1}{1 + f_v \chi_{0s}} \tag{28}$$

with $f_v = \frac{\delta^2 \epsilon_{xc}}{\delta m_v(\mathbf{r})^2} \frac{1}{\mu_s^2} < 0$. Thus if the exchange and correlation energy per particle depends explicitly on m_v, there is a valley exchange-correlation enhancement different from 1.

In standard local LDA/GGA functionals, the $SU(4)$ spin valley symmetry is broken and the exchange and correlation energy per particle is assumed to be

$$\epsilon_{xc} = \epsilon_{xc}(n, m) \tag{29}$$

independent of m_v. In this case, $f_v = 0$ and the valley exchange-correlation enhancement is exactly one. Thus the valley susceptibility is bare in this case.

Finally, it is important to remark that standard LDA/GGA parametrizations of the electron gas are for the three dimensional case. Thus the exchange-correlation enhancement of spin and valley susceptibilities is taken into account incorrectly.

Relation between phonon softening and bare susceptibility

The softening at $\mathbf{q}$ in Fermi liquid theory with an effective single particle potential [7] is written as:

$$\widetilde{\Delta\omega}_{\mathbf{q},\nu} = \frac{1}{N_k} \sum_k \frac{|\widetilde{d}^{\nu}_{\mathbf{k},\mathbf{k+q}}|^2}{\omega_{\mathbf{q},\nu}} \frac{f_{\mathbf{k+q}} - f_{\mathbf{k}}}{\epsilon_{\mathbf{k+q}} - \epsilon_{\mathbf{k}}} \tag{30}$$

the tilde means screened with respect to intervalley exchange correlation. Assuming a constant intervalley matrix element ($|d^{\nu}_{\mathbf{k},\mathbf{k+K}}| \approx |d^{\nu}_{\mathbf{K},\mathbf{2K}}|$), we have for the phonon softening at phonon momentum $\mathbf{q}$ close to $\mathbf{K}$:

$$\widetilde{\Delta\omega}_{\mathbf{q},\nu} = -\frac{|\widetilde{d}^{\nu}_{\mathbf{K},\mathbf{2K}}|^2}{2\omega_{\mathbf{q},\nu}} \chi_0(\mathbf{q}), \tag{31}$$

where the bare finite-momentum response-function is

$$\chi_0(\mathbf{q}) = -\frac{2}{N_k} \sum_k \frac{f_{\mathbf{k+q}} - f_{\mathbf{k}}}{\epsilon_{\mathbf{k+q}} - \epsilon_{\mathbf{k}}}. \tag{32}$$

For the parabolic 2-valley band-structure of Li_xZrNCl ad $\mathbf{q} = \mathbf{K}$ we have:

$$\widetilde{\Delta\omega_{\mathbf{K},\nu}} = -\frac{|\widetilde{d}^{\nu}_{\mathbf{K},\mathbf{2K}}|^2}{2\omega_{\mathbf{K}\nu}\mu_S^2} \chi_{0s}, \tag{33}$$

since $\chi_0(\mathbf{K}) = \lim_{\mathbf{q}\to\mathbf{K}} \chi_0(\mathbf{q}) = N(0) = \chi_{0s}/\mu_S^2$.

Electron-phonon interaction as a pseudo-magnetic field

In the basis $\{|\mathbf{K}+\boldsymbol{\kappa}\rangle, |\mathbf{2K}+\boldsymbol{\kappa}\rangle\}$, the most general Hamiltonian that describes the coupling with an intervally phonon of momentum $\mathbf{K}$ and branch index ν is:

$$H_{\mathrm{el-ph}} = \begin{pmatrix} 0 & d^{\nu}_{\mathbf{K}+\boldsymbol{\kappa},\mathbf{2K}+\boldsymbol{\kappa}} u_{\mathbf{K}\nu} \\ (d^{\nu}_{\mathbf{K}+\boldsymbol{\kappa},\mathbf{2K}+\boldsymbol{\kappa}})^* u_{\mathbf{K}\nu} & 0 \end{pmatrix} \tag{34}$$

where $d^{\nu}_{\mathbf{K}+\boldsymbol{\kappa},\mathbf{2K}+\boldsymbol{\kappa}}$ is the deformation potential and $u_{\mathbf{K}\nu}$ the amplitude of the phonon displacement. By writing

$$d^{\nu}_{\mathbf{K}+\boldsymbol{\kappa},\mathbf{2K}+\boldsymbol{\kappa}} = |d^{\nu}_{\mathbf{K}+\boldsymbol{\kappa},\mathbf{2K}+\boldsymbol{\kappa}}| e^{i\theta(\boldsymbol{\kappa})}, \tag{35}$$

we can obtain a real Hamiltonian by a redefinition of the basis, $|\mathbf{2K}+\boldsymbol{\kappa}\rangle \mapsto e^{-i\theta(\boldsymbol{\kappa})}|\mathbf{2K}+\boldsymbol{\kappa}\rangle$. In this new basis:

$$H_{\mathrm{el-ph}} = \begin{pmatrix} 0 & |d^{\nu}_{\mathbf{K}+\boldsymbol{\kappa},\mathbf{2K}+\boldsymbol{\kappa}}| u_{\mathbf{K}\nu} \\ |d^{\nu}_{\mathbf{K}+\boldsymbol{\kappa},\mathbf{2K}+\boldsymbol{\kappa}}| u_{\mathbf{K}\nu} & 0 \end{pmatrix}. \tag{36}$$

Finally, since intervalley matrix element is constant at small $\boldsymbol{\kappa}$, in the limit of small doping, we can ignore the $\boldsymbol{\kappa}$ dependence to obtain Eq. (3) of the main paper.

Phonon dispersion in Li_xZrNCl as a function of doping

In the case of constant matrix elements, the phonon softening is ruled by the bare response-function $\chi_0(\mathbf{q})$, see Eq. 31. Similarly the phonon linewidth is proportional to the nesting factor $N_f(\mathbf{q}) = \frac{1}{N_k}\sum_k \delta(\epsilon_{\mathbf{k}} - \epsilon_F)\delta(\epsilon_{\mathbf{k}+\mathbf{q}} - \epsilon_F)$. In Fig.6 (left) we plot $\omega_{\mathbf{K}} + \widetilde{\Delta\omega_{\mathbf{K}}}$ and the nesting factor (as vertical red bars) for a perfect parabolic 2D electron-gas. In the right panel, we compare these results with the DFT calculations for $x = 1/18$. At this doping, as well for $x = 1/9$ (see Fig. 7) the $2k_F$ area around $\mathbf{K}$ is well separated from that around Γ.

In the ideal case of constant intervalley matrix elements, the phonon softening is flat in a region of radius $2k_F$ around $\mathbf{K}$. Standard linear response calculations based on Fourier interpolation do not reproduce this fact (see Fig. 6 on the right, black dashed line) as the grid used in the calculation is too coarse. On the contrary the analytical behavior is very nicely captured by our Wannier interpolation scheme [7], as shown in Fig. 6 on the right, red lines. The simple model also accounts for the behavior of the phonon linewidth. In this case the nesting factor as a function of $\mathbf{q}$ of Fig.6 (left) should be compared with the phonon linewidth (red bars in Fig. 3 of the main paper).

The phonon dispersion and the Eliashberg functions for several doping are shown in Fig. 7. The intravalley contribution to the Eliashberg function and its integrated value are plotted on the left panels. As it can be seen the Eliashberg function is composed of two main peaks. The intravalley contribution to the electron-phonon coupling is suppressed for small doping.

* matteo.calandra@upmc.fr
† francesco.mauri@upmc.fr

[1] Y. Kasahara, T. Kishiume, T. Takano, K. Kobayashi, E. Matsuoka, H. Onodera, K. Kuroki, Y. Taguchi, and Y. Iwasa, *Enhancement of Pairing Interaction and Magnetic Fluctuations toward a Band Insulator in an Electron-Doped Li_xZrNCl Superconductor*, Phys. Rev. Lett. **103**, 077004 (2009), see Supplementary Informations.
[2] G. Vignale, M. Rasolt and D. J. W. Geldart, *Diamagnetic susceptibility of a dense electron gas*, Phys. Rev. B **37**
[3] G. Vignale, M. Rasolt,*Density-functional theory in strong magnetic fields*, Phys. Rev. Lett. **59**, 2360 (1987).
[4] Y. Zhang and S. Das Sarma, *Density-dependent spin susceptibility and effective mass in interacting quasi-two-dimensional electron systems*, Physical Review B, **72** , 075308 (2005)
[5] Ando T., Fowler A. B., and Stern F.,*Electronic properties of two-dimensional systems* Rev. Mod. Phys. **54**, 437 (1982)

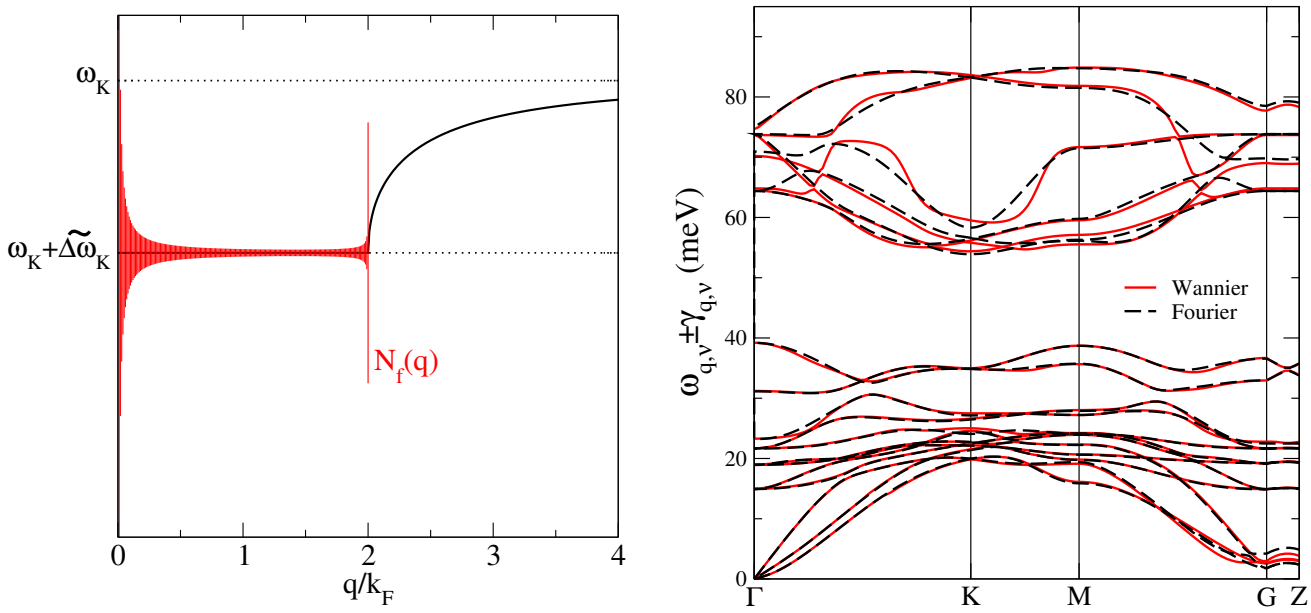

FIG. 6. (Left): Phonon frequency (black line) and line-width (vertical red bars) for a perfect parabolic 2D electron gas with constant electron-phonon matrix element. The phonon wavevector q is measured either with respect to zone center or with respect to **K**. (Right) : comparison between Wannier and Fourier interpolated phonon dispersion in $Li_{1/18}ZrNCl$.

[6] O. Gunnarsson and B. I. Lundqvist, *Exchange and correlation in atoms, molecules, and solids by the spin-density-functional formalism*, Phys. Rev. B **13**, 4274 (1976)

[7] M. Calandra, G. Profeta, and F. Mauri *Adiabatic and nonadiabatic phonon dispersion in a Wannier function approach* Phys. Rev. B **82**, 165111 (2010)

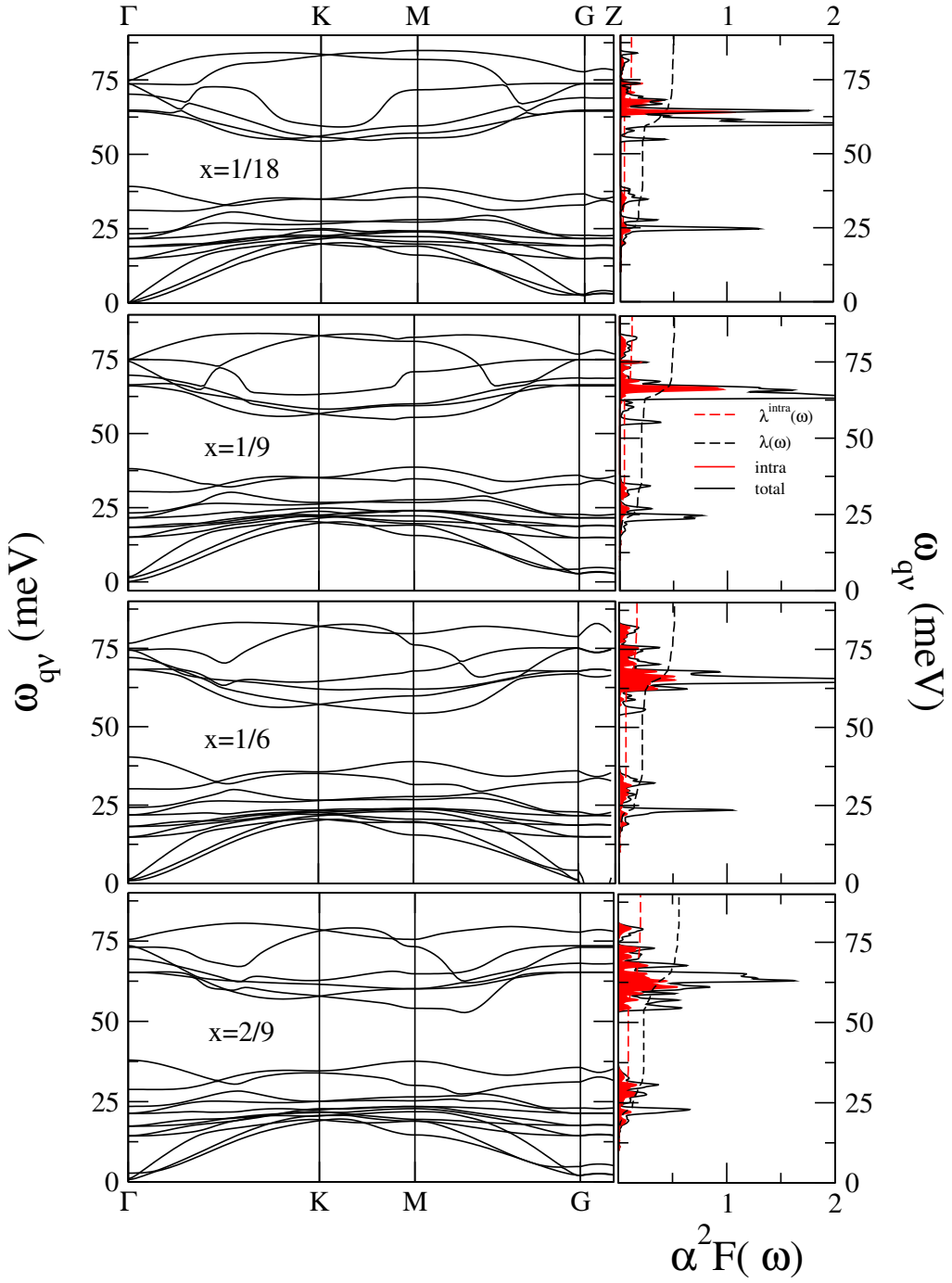

FIG. 7. Wannier interpolated phonon dispersion of Li_xZrNCl as a function of doping. The total Eliashberg function and the Eliashberg function due to intravalley scattering are also plotted on the right panels.